A neural network method for nonlinear hyperspectral unmixing

A NEURAL NETWORK METHOD FOR NONLINEAR HYPERSPECTRAL UNMIXING

Bikram Koirala, Rob Heylen, Paul Scheunders

Visionlab, University of Antwerp, Belgium

ABSTRACT

Because of the complex interaction of light with the Earth surface, a hyperspectral pixel can be composed of a highly nonlinear mixture of the reflectances of the materials on the ground. When nonlinear mixing models are applied, the estimated model parameters are usually hard to interpret and to link to the actual fractional abundances. Moreover, not all spectral reflectances in a real scene follow the same particular mixing model. In this paper, we present a supervised learning method for nonlinear spectral unmixing. In this method, a neural network is applied to learn mappings of the true spectral reflectances to the reflectances that would be obtained if the mixture was linear. A simple linear unmixing then reveals the actual abundance fractions. This technique is model-independent and allows for an easy interpretation of the obtained abundance fractions. We validate this method on several artificial datasets, a data set obtained by ray tracing, and a real dataset.

***Index Terms*—** Hyperspectral, neural networks, endmembers, abundances

1. INTRODUCTION

In hyperspectral unmixing, the aim is to estimate the fractional abundances of the different materials that are contained within the field of view of a pixel, by describing the obtained reflectance spectrum as a mixture of the reflectances of these materials. Because of the complex interaction of light with the Earth surface, spectral reflectances can be highly nonlinear mixtures of the reflectances of the materials on the ground, and nonlinear unmixing techniques are required.

In most cases, the reflectance spectra are modeled by a mixing model. When applying a mixing model, the fractional abundances of each endmember (material) in each pixel spectrum are estimated by inverting the model. This can be done by minimizing the error between the true spectrum and the reflectance spectrum that is reconstructed by using the specific mixing model.

The most common applied model is the linear mixing model (LMM), which is a valid model when the incoming rays of light interact with a single pure material in the instantaneous field of view (IFOV) before reaching the sensor. This model can be solved along with positivity and sum-to-one constraints on the abundances [1], using the Fully Constrained Least Squares Unmixing procedure (FCLSU).

Several nonlinear mixing models have been developed that try to model multiple interactions of the light with several pure materials. A popular group of models are the bilinear mixing models: the generalized bilinear model (GBM), the polynomial post-nonlinear model (PPNM), the linear quadratic model (LQM), and the Fan model (FM) as reviewed in [2]. Some recent models also consider more than two interactions, e.g. the multilinear mixing model (MLM) [3]. When intimate mixtures are in play, the Hapke model [2] can be applied.

When nonlinear mixing models are applied, the estimated model parameters are usually hard to interpret and to link to the actual fractional abundances. Moreover, not all spectral reflectances in a real scene follow the same particular mixing model. Some attempts have been made to learn a system to model the complex mixing effects rather than using specific mixing models. The methodology proposed by [4] learns a mapping from spectra to abundance fractions, which is basically a linear method. In [5], abundances obtained from a linear model were refined using a neural network-based forward modeling. In [6], artificial neural networks were used to decide whether a pixel is linearly or nonlinearly mixed, after which an appropriate model was applied for unmixing. This method however again requires the selection of particular nonlinear mixing models, which makes this method unreliable in real scenarios.

In this work, we propose a model-independent methodology that allows to estimate fractional abundances with high accuracy. The method requires a training set of spectral reflectances from which the endmembers and fractional abundances are known a priori. A neural network is then applied to train a mapping of the actual (nonlinear) spectral reflectances to a spectrum that is composed of a linear mixture. A simple linear unmixing then reveals the fractional abundances.

2. METHODOLOGY

Consider a set of p endmembers $\mathbf{E} = (\mathbf{e}_1, \mathbf{e}_2, \cdots, \mathbf{e}_p)$ in $\mathbf{R}_+^d$. In this work, we assume that the endmembers are either estimated from pure pixels in the data, or known a priori. Using a linear model, a spectrum $\mathbf{x}$ is described as a linear combi-

nation of these endmembers:

$$\mathbf{x} = \sum_{i=1}^{p} a_i \mathbf{e}_i + \boldsymbol{\eta} = \mathbf{E}\mathbf{a} + \boldsymbol{\eta} \quad (1)$$

along with the physical constraints: $\sum_i a_i = 1, \forall i : a_i \geq 0$. Here, $\mathbf{a} = (a_1, a_2, \cdots, a_p)$ are the fractional abundances for each endmember of the spectrum $\mathbf{x}$ and $\boldsymbol{\eta}$ represents Gaussian noise. Within this model, the endmembers define a simplex S_p in p-1 dimensions and all spectra that follow the model lie within that simplex.

In general, we can assume that any nonlinearity can be described by a nonlinear function $F(\mathbf{E}, \mathbf{a})$ of the endmembers and fractional abundances, i.e.:

$$\mathbf{x} = F(\mathbf{E}, \mathbf{a}) + \boldsymbol{\eta} \quad (2)$$

Instead of depending on a particular mixing model, for which a particular choice of F is fixed, we propose to apply a supervised method to learn F based on a training set of spectra with known fractional abundances. From the available abundance and endmember information of each of the training spectra $\mathbf{x}$, we generate linearly mixed spectra $\mathbf{x}_l$:

$$\mathbf{x}_l = \mathbf{E}\mathbf{a} + \boldsymbol{\eta} \quad (3)$$

A neural network is then trained to learn a mapping of the spectrum of the actual training spectra $\mathbf{x}$ to the linearly mixed spectra $\mathbf{x}_l$. The network architecture is a multilayer perceptron (MLP) such that the input layer contains the spectral bands of the actual spectra $\mathbf{x}$ (d nodes) and the output layer is of the same size and contains the spectral bands of the generated linear spectrum $\mathbf{x}_l$. One or more hidden layers are placed in between. Once the mapping is generated, an unknown spectrum can be introduced to the network, and the generated output spectrum can simply be unmixed by applying FCLSU, obtaining the fractional abundances.

The neural network applied in this work has three layers: the d-band input layer, a hidden layer consisting of 10 nodes, and the d-band output layer. To train the network, the Levenberg-Marquardt backpropagation [7] training algorithm was used. The training was performed by dividing the dataset into three categories: a training, a validation, and a test set. The training set was used to determine the network parameters (weights and biases) while the validation set was used to minimize the generalization error (over-fitting).

3. EXPERIMENTAL RESULTS AND DISCUSSION

3.1. Simulated data

In the first experiment, seven different mixing models: LMM, GBM, PPNM, LQM, FM, the Hapke model, and MLM were used simultaneously to generate reflectance spectra. The parameters and constraints of these models are listed in Table 1. Three endmembers were randomly chosen from the USGS database, containing 224 reflection values for wavelengths in the range 0.383-2.508 μm. Abundances were generated uniformly and randomly from the unit simplex. On all generated spectra, Gaussian noise was added with SNR = 20 dB.

To train the neural network, we generated 700 pixels (100 pixels from each mixing model). From the 700 pixels, 315 pixels were used for training and 35 pixels were used for validation. After training was completed, the test dataset (350 pixels) was unmixed using FCLSU. Table 2 shows the abundance root mean squared errors (RMSE) for the seven different mixing models and our methodology. This result demonstrates that the neural network is able to learn the mappings of several models simultaneously.

3.2. Samson data

In the second experiment, we used the Samson dataset provided by [8] which is available at this webpage:
`http://www.escience.cn/people/feiyunZHU/Dataset_GT.html`.
This data contains three endmembers (tree, rock, and water). These endmember comprise 156 reflection values for wavelengths in the range 0.401-0.889 μm. For this dataset, ground reference data was prepared for a (95×95) pixels subset of the image. We used 180 pixels for training and 20 pixels for validation. The trained network was applied to the remaining 8825 pixels.

Figure 1 displays the ground truth, the estimated abundance maps and the absolute difference between the ground truth and estimated abundance maps obtained by MLM and our method. Table 2 shows the abundance RMSE for the seven different mixing models and our methodology.

3.3. Ray tracing data

In the final experiment, the ray tracing datasets (orchard scenes), generated by [9] were used. This dataset is synthetic but highly resembles true hyperspectral images. The fully calibrated virtual citrus orchard, developed in [10] was used to generate two scenes: an orchard with mixtures of 2 endmembers: citrus trees and soil, and an orchard with mixtures of three endmembers: citrus trees, soil and weed patches. These orchard scenes contain 20×20 pixels and each pixel has a size of 2 m $\times$ 2 m. The exact per pixel abundances and endmember spectra are provided. From the 400 pixels, we used 40 pixels for training, 20 pixels for validation and the remaining 340 pixels for testing.

Figure 2 displays the ground truth, the estimated abundance maps and the absolute difference between the ground truth and estimated abundance maps obtained by the Hapke model and our method, in the three endmember case. Table 2 shows the obtained abundance RMSE for the seven different mixing models and our methodology. The obtained results show the superior performance of our method compared to the LMM, the bilinear models, the multilinear model and the Hapke model.

Model	Equation	Parameters
Linear	$\mathbf{x} = \sum_{i=1}^{p} a_i \mathbf{e}_i$	
GBM	$\mathbf{x} = \mathbf{y} + \sum_{m=1}^{p-1} \sum_{k=m+1}^{p} b_{mk} \mathbf{e}_m \odot \mathbf{e}_k$ $\mathbf{y} = \sum_{i=1}^{p} a_i \mathbf{e}_i$	$\forall m \geq k : b_{mk} = 0$ $\forall m < k : b_{mk} = \gamma_{mk} a_m a_k, \gamma_{mk} \in [0, 1]$
PPNM	$\mathbf{x} = \mathbf{y} + b(\mathbf{y} \odot \mathbf{y})$ $\boldsymbol{y} = \sum_{i=1}^{p} a_i \mathbf{e}_i$	$\forall m, k : b_{mk} = b a_m a_k$ $b \in [-0.25, 0.25]$
LQM	$\mathbf{x} = \mathbf{y} + \sum_{m=1}^{p} \sum_{k=1}^{p} b_{mk} \mathbf{e}_m \odot \mathbf{e}_k$ $\mathbf{y} = \sum_{i=1}^{p} a_i \mathbf{e}_i$	$\forall m, k : b_{mk} \geq 0$
FM	$\mathbf{x} = \mathbf{y} + \sum_{m=1}^{p-1} \sum_{k=m+1}^{p} b_{mk} \mathbf{e}_m \odot \mathbf{e}_k$ $\mathbf{y} = \sum_{i=1}^{p} a_i \mathbf{e}_i$	$\forall m \geq k : b_{mk} = 0$ $\forall m < k : b_{mk} = a_m a_k$
Hapke	$x = \frac{w}{(1 + 2\mu\sqrt{1-w})(1 + 2\mu_0\sqrt{1-w})}$ $\sqrt{1-w} = \frac{\sqrt{(\mu_0+\mu)^2 x^2 + (1+4\mu_0\mu x)(1-x)} - (\mu_0+\mu)x}{1+4\mu_0\mu x}$	μ_0: cosine incident angle μ: cosine reflectance angle
MLM	$\mathbf{x} = \frac{(1-P)\mathbf{y}}{1-P\mathbf{y}}, \mathbf{y} = \sum_{i=1}^{p} a_i \mathbf{e}_i$	$P \in [0, 1]$

Table 1: Linear and nonlinear models and their parameters. The assumption for all models: $\forall m : a_m \geq 0, \sum_m a_m = 1$.

Model	Simulated	Samson	Ray tracing
LMM	9.21	41.73	17.80
FM	10.02	40.64	15.07
GBM	9.32	41.73	14.72
PPNM	8.51	38.97	16.20
LQM	12.13	41.73	22.15
MLM	11.55	18.34	19.02
Hapke	16.07	45.80	8.81
Our method	**5.09**	**2.24**	**2.05**

Table 2: Abundance RMSE ($\times 10^{-2}$) for the simulated, Samson, and the ray tracing dataset.

4. CONCLUSION

In this paper, we proposed a supervised method for nonlinear hyperspectral unmixing. A neural network is applied to learn the mapping of a nonlinear spectrum to the corresponding linear one, composed of the same fractional abundances. This method not only maps the nonlinear effects but also solves the interpretation problem of the estimated abundances. Experiments on simulated, true and ray tracing datasets show that the performance of this novel methodology is very promising.

The proposed method is model-independent, but has an important disadvantage over the use of nonlinear models, in that it requires a training set. Acquiring high quality ground reference data for hyperspectral mixed data is not straightforward. On the other hand, once a network is trained, it can be applied on similar datasets (i.e. with the same endmembers). In case of endmember variability, the assumption of fixed endmembers will be violated. Endmember variablity can however in principle be trained along with the mapping. This is the topic of our current research.

5. REFERENCES

[1] J. W. Boardman, "Geometric mixture analysis of imaging spectrometry data," in *Geoscience and Remote Sensing Symposium, 1994. IGARSS '94. Surface and Atmospheric Remote Sensing: Technologies, Data Analysis and Interpretation., International*, Aug 1994, vol. 4, pp. 2369–2371 vol.4.

[2] R. Heylen, M. Parente, and P. Gader, "A review of nonlinear hyperspectral unmixing methods," *IEEE Journal of Selected Topics in Applied Earth Observations and Remote Sensing*, vol. 7, no. 6, pp. 1844–1868, June 2014.

[3] R. Heylen and P. Scheunders, "A multilinear mixing model for nonlinear spectral unmixing," *IEEE Transactions on Geoscience and Remote Sensing*, vol. 54, no. 1, pp. 240–251, Jan 2016.

[4] PM Atkinson, MEJ Cutler, and H Lewis, "Mapping subpixel proportional land cover with avhrr imagery," *International Journal of Remote Sensing*, vol. 18, no. 4, pp. 917–935, 1997.

[5] Sadegh Karimpouli, Amir Salimi, and Saeid Ghasemzadeh, "Seminonlinear spectral unmixing using a neural network-based forward modeling," *Journal of Applied Remote Sensing*, vol. 10, no. 3, pp. 036006–036006, 2016.

[6] Asmau M Ahmed, Olga Duran, Yahya Zweiri, and Mike Smith, "Hybrid spectral unmixing: using artificial neural networks for linear/non-linear switching," *Remote Sensing*, vol. 9, no. 8, pp. 775, 2017.

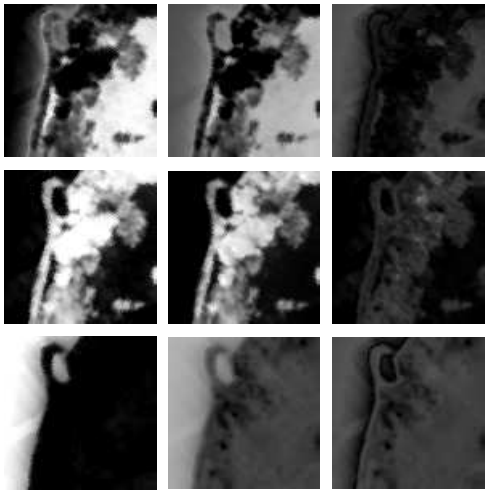

(a) MLM

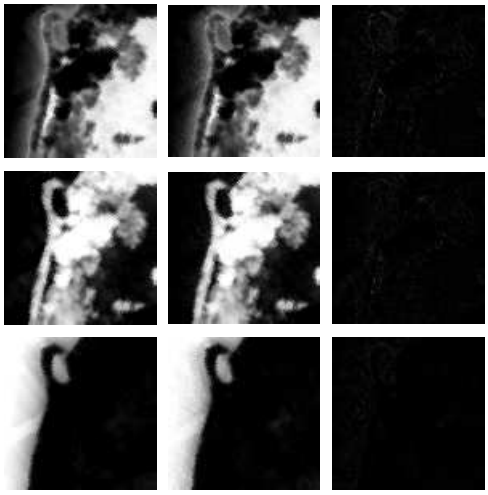

(b) our method

Fig. 1: Abundance maps from the Samson data set. Rows 1, 2 and 3 denote rock, tree and water. From left to right: the ground truth, the estimated abundance map, the absolute difference between estimated and ground truth abundance maps.

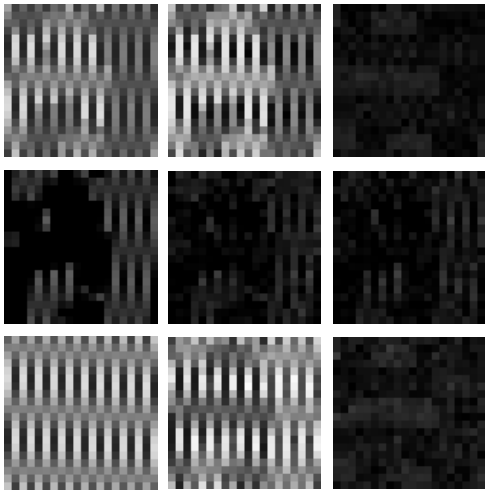

(a) Hapke

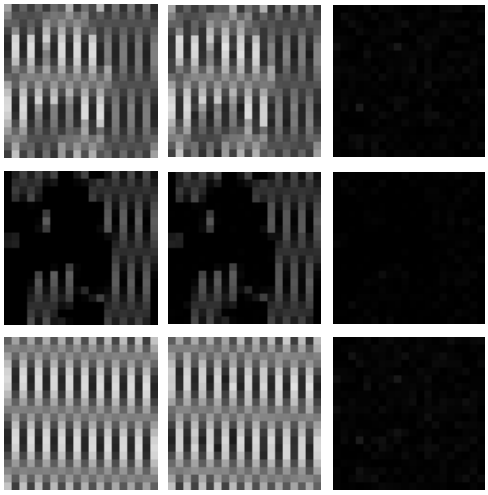

(b) our method

Fig. 2: Abundance maps from the ray tracing data set. Rows 1, 2 and 3 denote soil, weed and tree. From left to right: the ground truth, the estimated abundance map, the absolute difference between estimated and ground truth abundance maps.

[7] Donald W Marquardt, "An algorithm for least-squares estimation of nonlinear parameters," *Journal of the society for Industrial and Applied Mathematics*, vol. 11, no. 2, pp. 431–441, 1963.

[8] Feiyun Zhu, Ying Wang, Bin Fan, Shiming Xiang, Geofeng Meng, and Chunhong Pan, "Spectral unmixing via data-guided sparsity," *IEEE Transactions on Image Processing*, vol. 23, no. 12, pp. 5412–5427, 2014.

[9] B. Somers, L. Tits, and P. Coppin, "Quantifying nonlinear spectral mixing in vegetated areas: Computer simulation model validation and first results," *IEEE Journal of Selected Topics in Applied Earth Observations and Remote Sensing*, vol. 7, no. 6, pp. 1956–1965, June 2014.

[10] Jan Stuckens, Ben Somers, Stephanie Delalieux, WW Verstraeten, and Pol Coppin, "The impact of common assumptions on canopy radiative transfer simulations: A case study in citrus orchards," *Journal of Quantitative Spectroscopy and Radiative Transfer*, vol. 110, no. 1, pp. 1–21, 2009.